A Turbulent Jet Flame Stabilized on a Thick Burner Rim

Kenichi ITOH*
Masafumi SASAKI*

(Received June 30, 1976)

Abstract

The stabilization of propane-air premixed jet flames in a high velocity parallel air flow was investigated experimentally. The burner tubes has an 8 mm inner diameter with rims of 0–7 mm thickness. The flame was stabilized in a higher velocity and turbulent flow region where the rim is of sufficient thickness. The recirculation zone forming behind the thick rim had strong influences on the flame stability. In this jet flame the aerodynamic and thermodynamic characteristics of the recirculation zone were not independent from each other, because the entrainment of the parallel air into the wake zone changed the chemical composition of the zone. Mixing processes in the reciaculation zone, which determined the true mixing ratio of the zone, were obtained experimentally with CO_2 trace methods.

1. Introduction

It is well known that the air flow around a burner tube has a strong influence on the stability limits of a Bunsen flame[1),2)]. One typical example of Bunsen flame with surrounding air flow is the double concentric jet formation, the center round jet is fuel or mixture and the coaxial annular jet is a parallel air flow. Generally, parallel air flow disturbs the flame.

On the other hand, if the burner rim is of sufficient thickness a recirculation zone is formed on the rim by parallel air flow. The flames are stabilized in a higher velocity region within this recirculation zone. Such phenomenona have been reported by Saima[3)]. In such flames, the thermodynamic characteristics are determined after more complex processes, exchange of the air and mixture, and change of chemical composition in the recirculation zone, in comparison with the flames stabilized by the recirculation zone behind a bluff body situated in uniform mixture flow.

In this paper, general properties of such premixed flames, and structures of the recirculation zone which has influences on the flame stability were investigated experimentally. And the mixing processes of mixture and parallel air in the recirculation zone were examined.

* Department of Mechanical Engineering, Faculty of Engineering, Hokkaido University, Sapporo, Japan.

2. Experimental apparatus

A schematic diagram of the experimental apparatus is shown in Fig. 1. Fuel is pure LPG (C_3H_8, purity 97%), and is premixed with the primary air in the mixing chamber. The mixture is carried to a round brass burner set coaxially in the glass combustion tube which has a diameter of 55 mm and a length of 1700 mm. The parallel air flow surrounds the burner tube. Velocity of mixture U_{mix} and of the parallel air U_2 can be controlled up to 70 m/s and 30 m/s, respectively. Thicknesses of the rim at each burner tip t are 0, 1.5, 3, 5, 7 mm, and the inner diameter of all burners is 8 mm as shown in Fig. 2.

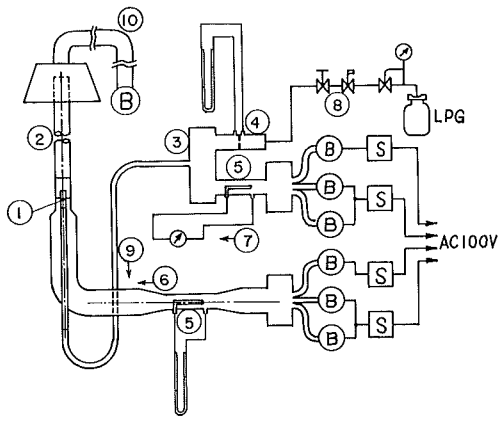

Fig. 1. Schematic diagram of experimental apparatus

1. Burner tube
2. Combustion tube
3. Maxing chamber
4. Orifice
5. Pitot tube
6. Secondary air
7. Primary air
8. Fuel
9. Mixture
10. Exhaust duct

B; Blower S; Variable voltage trans.

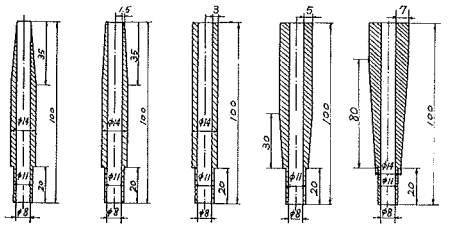

i) $t=0$ ii) $t=1.5$ iii) $t=3$ iv) $t=5$ v) $t=7$ mm

Fig. 2. Geometries of burner tips.

3. Flame stability limits and flame geometries

3.1 Flame geometries

A flame stability limit is shown in Fig. 3 in axes of primary velocity U_{mix} and mixing ratio ϕ (air/fuel)/(air/fuel)$_{st.}$. The larger ϕ is, the leaner fuel ratio becomes. Blow out is defined as extinguishment of the flame, and flash back limit is not obtained. Flames are formed between the upper limit line and the lower limit line in the figure. The forms of the flames are mainly distinguished into two types, the inner flame (A region) and the outer flame (B region), by the position of the flame front in the recirculation zone formed behind the burner rim. Flame fronts in the flame base are located near the inner and the outer circumferences in the inner flame and the outer flame, respectivelly.

On the boundary of the inner flame and the outer flame, the flame is a transitional form of the two. In this flame, referred to as transitional flame, the flame fronts are formed near both the inner and the outer circumferences of the rim, or a repetition of each form is seen. But the flame front never formed on the inside of the recirculation zone.

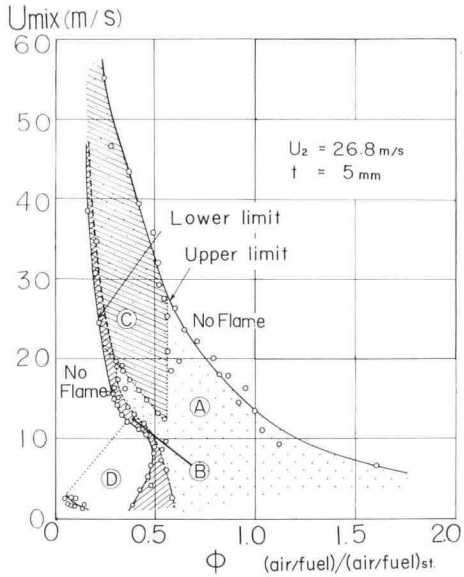

Fig. 3. Inflamable region.

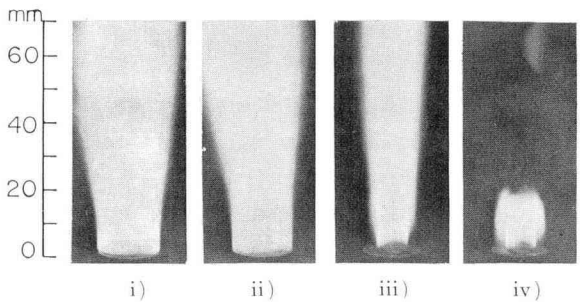

Fig. 4. Photographs of flame geometries
i) Outer flame iii) Inner flame
ii) Transitional flame iv) Crown flame

In C region, the flame stays only in the recirculation zone, and the remainder, or the main flame, blows off. This is referred to as crown flame and was also reported by Saima[3] and Matsumoto et al.[4]. Almost all of the mixture is unburned, because of extinguishment of the main flame. The crown flame is also divided into the inner and the outer flame.

In D region, the parallel air enters the center jet inversely, because U_2 exceeds U_{mix} by far. Luminous flame can be seen in the inside the flame. This is called reverse flame.

Fig. 4 shows these flame geometries.

3.2 The flame stability limits without the parallel air flow or the thickness of rim

The stability limits when there is no forced flow around the center jet is

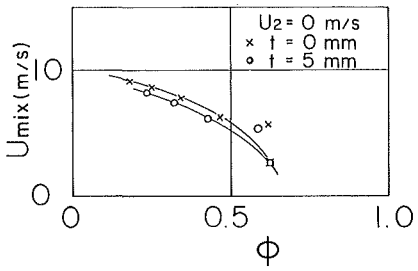

Fig. 5. Stability limits ($U_2=0$).

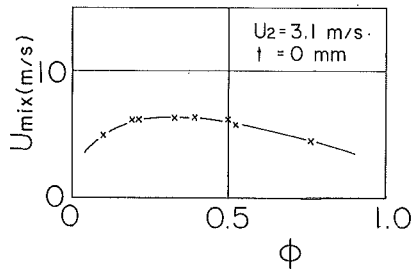

Fig. 6. Stability limits ($t=0$).

shown in Fig. 5. These results are in good agreement with other papers[5),6)]. The upper limit is roughly independent of the thickness of the rim t. On the other hand, the stability limit with the parallel flow at $t=0$ is shown in Fig. 6. The limit is lower than that without the parallel flow especially where ϕ is small. When $U_2 \geqq 6$ m/s, the flame can not be maintained.

3.3 Effects of the thickness of rim on the stability limits

Changes of the stability limits against t are shown in Fig. 7. Difference between limits when $t=0$ and $t=1.5$ mm is not so noticeable. But when $t \geqq 3$ mm, the flame can be stabilized in a higher mixture velocity region. Generally, when t is sufficiently thick the upper limit moves to larger (leaner) ϕ and maximum blow out mixture velocity increases as t increases.

3.4 Effects of the velocity of the parallel air flow on stability limits

When t is sufficiently thick the blow out limit shifts in direction of larger ϕ and maximum blow out mixture velocity increases by increasing U_2. These results are shown in Fig. 8. Increasing rate of the upper limit is smaller than that of the lower limit.

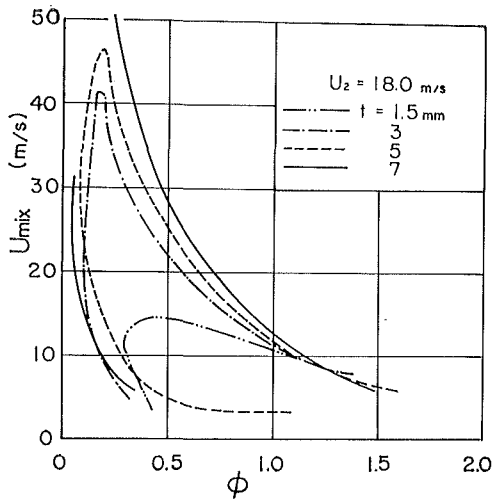

Fig. 7. Effects of t on stability limits.

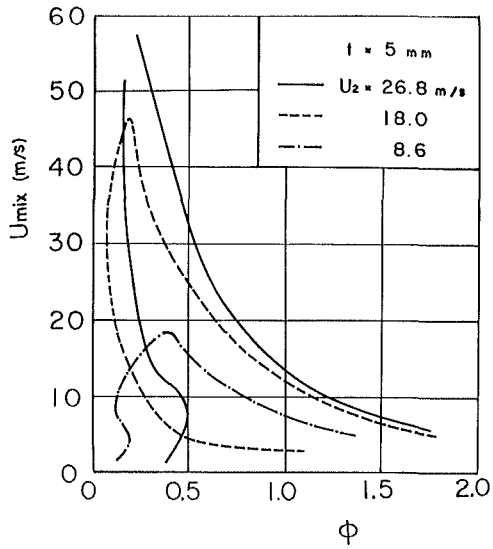

Fig. 8. Effects of U_2 on stability limits.

3.5 Roles of the flame base

In the crown flame, combustion occurs only at the flame base and the main flame blows off. Although the transition to crown flame from normal flame (with the main flame) is abrupt, the boundary between the sphere of each form is shown clearly in Fig. 3. Each upper and lower limit line is also continuous near the boundary. It shows that blow out is defined by extinguishing of the flame at the flame base irrespective of the crown flame or normal flame. Therefore, it is suggested that the structures of the flame base have a strong effect on the flame stability.

The flame base mainly consists of the recirculation zone, and acts as a heat source for the unburned mixture, as well as the recirculation zone formed behind a bluff body settled in mixture flow. In a round jet flame with parallel air flow, however, the chemical composition of the recirculation zone is changed by the entrainment of the parallel air.

The stability mechanism of the double concentric jet flame differs from that of the flame held by the bluff body. To clarify the structures of the recirculation zone in this model, aerodynamically and thermodynamically, and discussion of the mechanism of the flame stability is required.

4. The aerodynamic characteristics of the recirculation zone

4.1 The length of the recirculation zone

On the flames held by a bluff body, or a recessed wall settled in uniform mixture flow, the stability mechanism based on the ignition delay concept[7),8)] is well known. According to this theory, the length of the recirculation zone l_{RZ} is one of the most important factors. In this paper, l_{RZ} is measured by flame reaction of sodium. The length measured by this method includes not only the recirculation zone, but also the reverse flow zone out of the recirculation zone. When $t \leqq 1.5$ mm, the reverse flow zone could not be found with this method. Fig. 9 shows the relation of l_{RZ} and U_{mix} when $t \geqq 3$ mm, l_{RZ} decreases as U_{mix} increases, and increases as t and U_2 increases. And it can be said that l_{RZ} does not depend on ϕ, but only depends upon the aerodynamic processes.

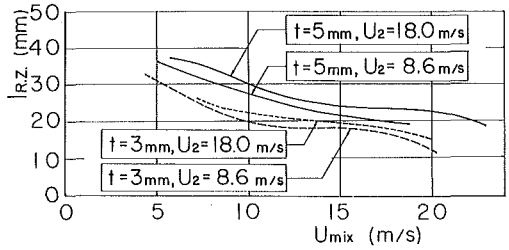

Fig. 9. Change of l_{RZ} vs U_{mix}.

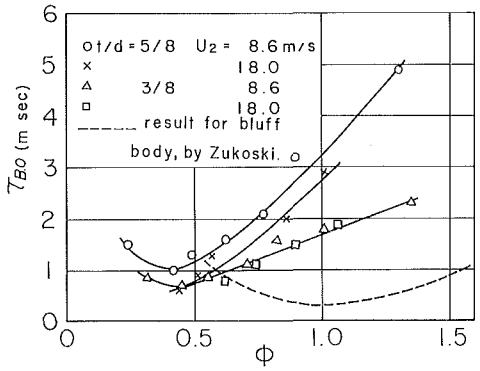

Fig. 10. Critical ignition delay time.

The critical ignition delay time τ_{BO} obtained by the ignition delay concept is shown in Fig. 10 as a relation of ϕ. The very ϕ which brings minimum τ_{BO} is smaller than unity, and the minimum τ_{BO} is two or three times larger in comparison with the results which E. E. Zukoski obtained for a bluff body. It is considered that the differences arise from entrainment of parallel air into the recirculation zone, so the theory cannot be applied to this experiment.

4.2 Schematic flow pattern near the recirculation zone

It is necessary for the flow pattern of the recirculation zone to be measured to understand the aerodynamic structure of the recirculation zone. In this experiment, however, turbulence in the recirculation zone is so intensive, and the zone is so small that it is difficult to visualize the flow pattern or to measure it accurately. Fig. 11 shows the rotary total pressure probe which has a total pressure hole on the rotary axis. The probe for cold flow is made of stainless tubing (diameter of 1 mm) and has a hole of 0.3 mm diameter, and for combustion flow the probe is made of a quartz glass tube (diameter of 1 mm) and has 0.2 mm hole opened with ultra sonic machining. These probes are inserted perpendicularly to the measuring face. And it is concidered that the direction of the hole which gives the maximum total pressure is the reverse direction of the flow.

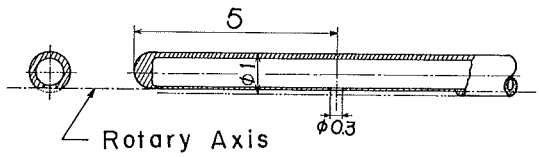

Fig. 11. Tip geometry of rotary total pressure probe.

Extreme transformations of the schematic flow pattern can be observed as U_{mix} and U_2 change, as shown in Fig. 12. In a), U_{mix} is much smaller than U_2 and the reverse flow of the parallel air is formed on the burner axis. That is called reverse vortex. In b), there is one vertex rotating from inside to outside on the burner rim, which is called inner vortex.

In c), there are two opposing vortexes, which are referred to as double vortex. In d), there is one vortex from the outside to the inside, referred to as the outer vortex. These transformations of the flow pattern are formed in the order named (a)→(d) as U_{mix} increases. The order is the same at different U_2. For it is considered that the transformations of the flow pattern are concerned with the entrainments of both U_{mix} and U_2, the forms of vortex may be ordered by the velocity ratio U_{mix}/U_2, as shown in Fig. 13. The figure shows that the form of the vortex is roughly determined by U_{mix}/U_2 whenever U_2 is changed. When with combustion flow, the length of the reverse flow zone extends to 1.5–2 times in comparison with that with a cold flow. But the direction of flow itself does not differ from that with a cold flow.

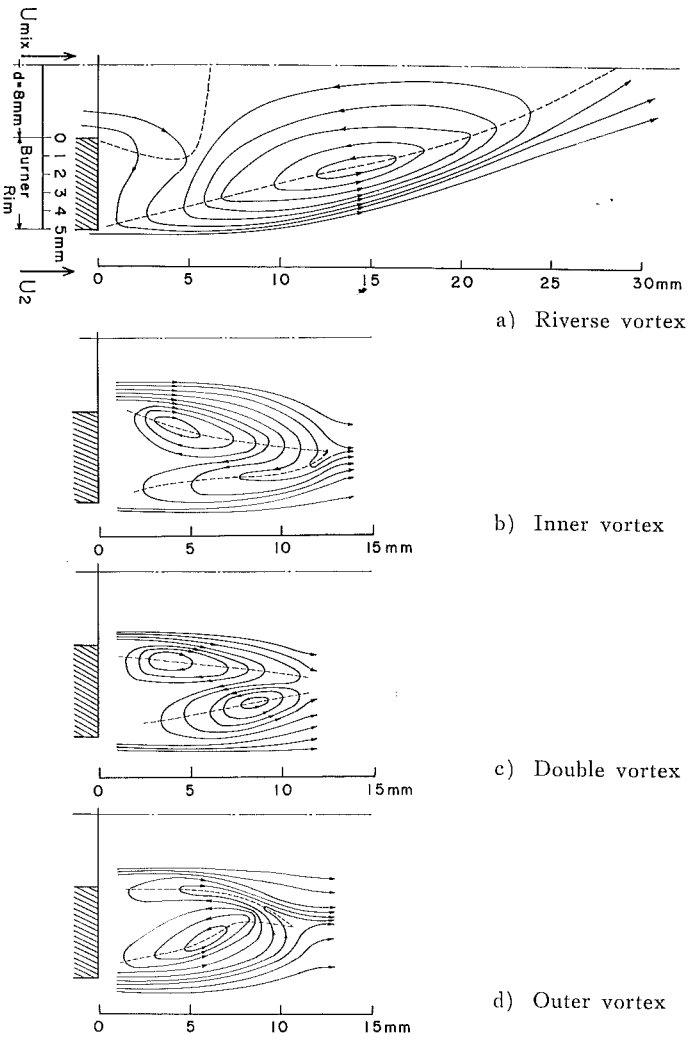

Fig. 12. Schematic flow patterns

a) Reverse vortex; U_{mix}= 5.0 m/s, U_2=26.8 m/s, t/d=5/8 with cold flow.
b) Inner vortex ; U_{mix}=13.0 m/s, U_2=18.0 m/s, t/d=5/8 with cold flow.
c) Double vortex ; U_{mix}=18.0 m/s, U_2=18.0 m/s, t/d=5/8 with cold flow.
d) Outer vortex ; U_{mix}=48.0 m/s, U_2=18.0 m/s, t/d=5/8 with cold flow.

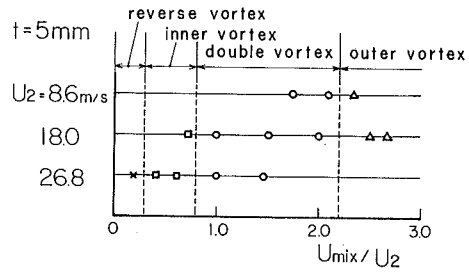

Fig. 13. Change of flow pattern against U_{mix}/U_2.

4.3 Static pressure distribution near the recirculation zone

Static pressure distribution is also one of the most important factors to show flow field. In this experiment, the static pressure probe which has a hole (diameter of 0.3 mm) opened prependicular to a thin rectangular plate (3×3 mm, thickness of 0.2 mm) is used only with cold flow. Although there is but a little swirl, and much difficulty is encountered in setting up the probe, the tendencies of distribution, for instance, the static pressure gradient showed a sufficiently reliable reappearance. A typical static pressure distribution is shown in Fig. 14. The form of the vortex can not be directly discriminated by static pressure distribution. Generally, the pressure gradient, especially through the axis, becomes sharper and the minimum pressure on the rim decreases as U_{mix} increases. The minimum pressure region on the rim includes the vortex center. Although it is not shown in Fig. 14, the maximum pressure region is formed downstream of the minimum pressure region. This maximum region is located on the burner axis when U_{mix} is sufficient. The phenomenon was also reported by Chigier et al.[9].

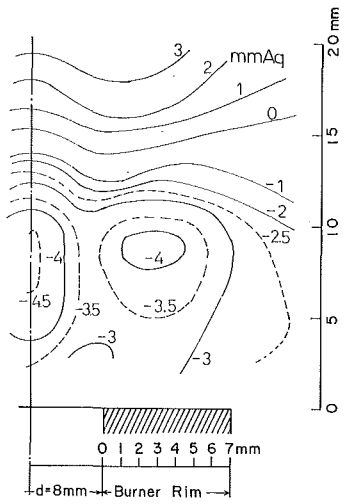

Fig. 14. Static pressure distribution
$U_{mix}=27.0$ m/s, $U_2=18.0$ m/s, $t/d=7/8$ with cold flow.

5. The thermodynamic characteristics of the recirculation zone

5.1 Temperature distribution and concentration distribution of gas components in the recirculation zone

Temperature of the flame is measured by Pt–PtR 13% thermocouple which is inserted into the flame. Errors arising from radiation from the tip of the thermocouple was not compensated for. Gas components in the recirculation zone are sampled with a quartz glass tube (diameter of 0.3 mm) and each component is measured by gas-chromatography.

Temperature- and concentration- distribution of the outer flame is as shown in Fig. 15, and that of the stable inner flame is as shown in Fig. 16, and that of the inner flame near the upper limit is as shown in Fig. 17. Generally, the maximum temperature region (≧1400°C) and minimum concentration region of O_2 and maximum concentration region of CO_2 roughly overlap. The maximum temperature region is located just inside of the flame front, or overlap with the flame front in the outer flame. On the other hand, the maximum temperature region is located outside of the flame front in the inner flame, and moves to the flame front as the flame approaches the upper blow out limit. CO is distributed over the entire recirculation zone in the stable inner flame, but only near the

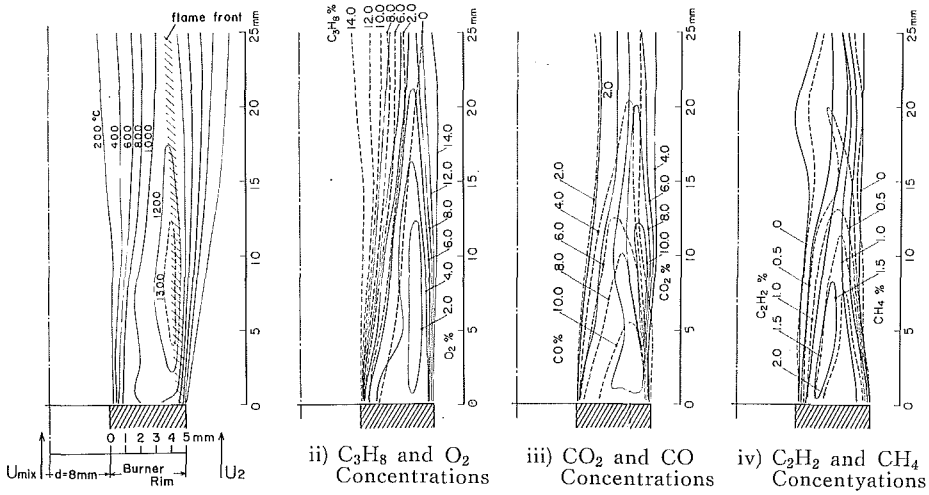

i) Temperature ii) C_3H_8 and O_2 Concentrations iii) CO_2 and CO Concentrations iv) C_2H_2 and CH_4 Concentyations

Fig. 15. Temperature and Concentration distribution of outer flame $U_{mix}=15.2$ m/s, $U_2=26.8$ m/s, $\phi=0.30$, $t/d=5/8$.

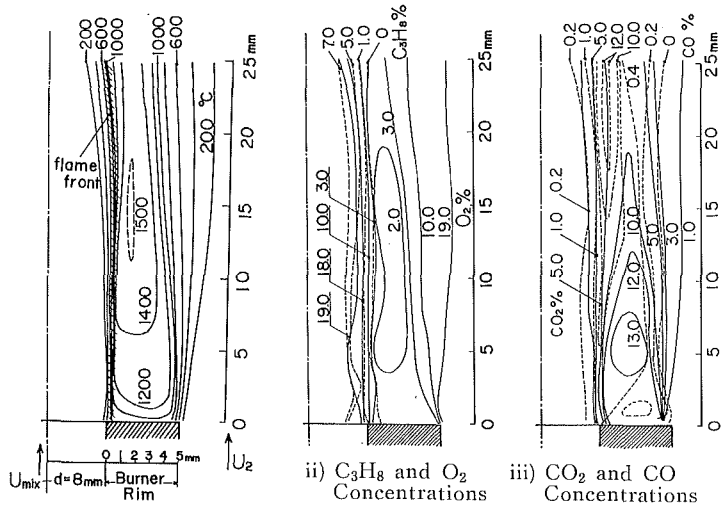

i) Temperature ii) C_3H_8 and O_2 Concentrations iii) CO_2 and CO Concentrations

Fig. 16. Temperature and Concentration distribution of stable inner flame $U_{mix}=10.8$ m/s, $U_2=26.8$ m/s, $\phi=0.64$, $t/d=5/8$.

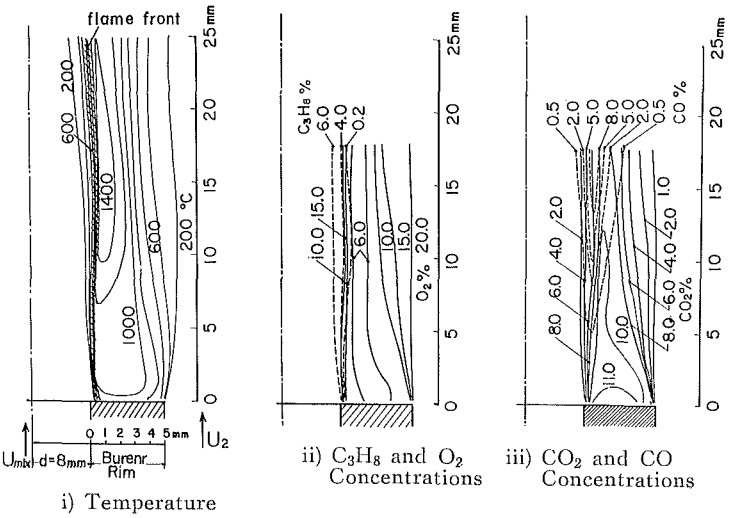

i) Temperature ii) C_3H_8 and O_2 Concentrations iii) CO_2 and CO Concentrations

Fig. 17. Temperature and Concentration distribution of inner flame near the upper limit $U_{mix}=23.3$ m/s, $U_2=26.8$ m/s, $\phi=0.64$, $t/d=5/8$.

flame front in the inner flame near the upper limit. And O_2 concentration increases as the flame approaches the upper limit. Thus it is suggested that the entrainment of the parallel air into the recirculation zone increases for the same ϕ, as U_{mix} increases.

5.2 Local mixing ratio distribution and position of flame front

Gas components and local mixing ratio ϕ_{local} distribution at the section of 3 mm downstream from the edge of the burner, is shown in Fig. 18. Almost only CO and H_2 are burned at the flame front in the outer flame. In the inner flame, rapid reaction of C_3H_8 is carried out. Many intermediate products (much CH_4, C_2H_2, a little C_2H_4, C_2H_6) are distributed above the burner rim in the outer flame, but bardly any is found in the inner flame. Local mixing ratio ϕ_{local} is distributed almost uniformly in the recirculation zone, and when viewed in detail, the position of the flame front is found to be located in the same position of $\phi_{local}=1.0$ for every flame (outer flame (i), transitional flame (ii) and inner flame (iii)). It can be concluded that the flame front is formed on the position of $\phi_{local}=1.0$. This phenomenon agrees with the results of the diffusion flame held by disk as reported by E. Minx et al.[10]. The form of flame is consequently determined by the true mixing ratio, which is different from that of mixture, in the recirculation zone.

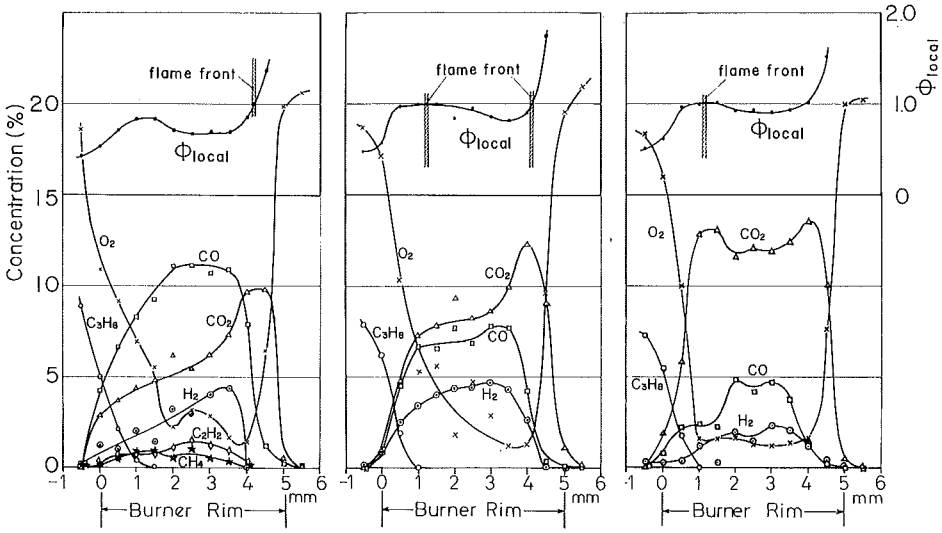

Fig. 18. Local mixing ratio distribution

i) Outer flame ; $U_{mix}=11.0$ m/s, $U_2=26.8$ m/s, $\phi=0.40$, $t/d=5/8$.
ii) Transitional flame; $U_{mix}=11.0$ m/s, $U_2=26.8$ m/s, $\phi=0.45$, $t/d=5/8$.
iii) Inner flame ; $U_{mix}=11.4$ m/s, $U_2=26.8$ m/s, $\phi=0.52$, $t/d=5/8$.

6. Mixing processes in the recirculation zone

As stated above, a large part of the behaviour of the flame has a strong dependence on the mixing processes of the mixture and the parallel air in the recirculation zone. Namely, thermodynamic processes, and aerodynamic processes, which are independent of each other for the flame held by a bluff body settled in a uniform mixture stream, are closely concerned with each other by mixing processes.

6.1 Constant ϕ_{RZ} diagram

Using CO_2 as a tracer instead of fuel, the resulting distribution by diffusion of mixture can be readily investigated with a cold flow. The CO_2 concentration distribution is as shown in Fig. 19. Concentration in the recirculation zone is almost uniform except for the region in which U_{mix} is much smaller than U_2. Then the mean mixing ratio in the recirculation zone ϕ_{RZ} can be represented by the value of one point inside the zone, and therefore the fluctuation of ϕ_{RZ} by U_{mix} and ϕ for the same t, U_2 can be easilly examined. Constant ϕ_{RZ} diagram, which is $U_{mix}-\phi$ plane on which constant ϕ_{RZ} curves are drawn, may be a characteristic diagram of mixing in a double concentric jet. The representative measurement position of ϕ_{RZ} (z, r) is (3, 2) and (2, 1.5) (mm) at $t=5$ and $t=3$ mm, respectively, where r is at a radial distance from the inner circumference and z is the axial distance from the burner rim. Fig. 20 shows the constant ϕ_{RZ} diagram overlapping with the inflamable region (the shadowed region). Both limit lines and the constant ϕ_{RZ} curves have the same tendency, that is, they have a similar

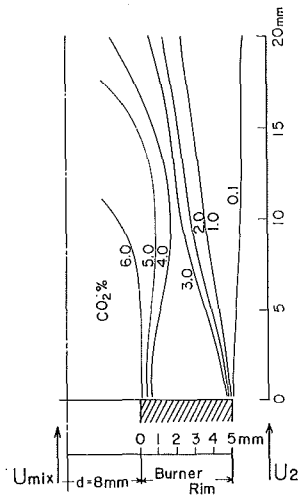

Fig. 19. Concentration distribution of mixture

$U_{mix}=16.3$ m/s, $U_2=26.8$ m/s, $t/d=5/8$ with cold flow.

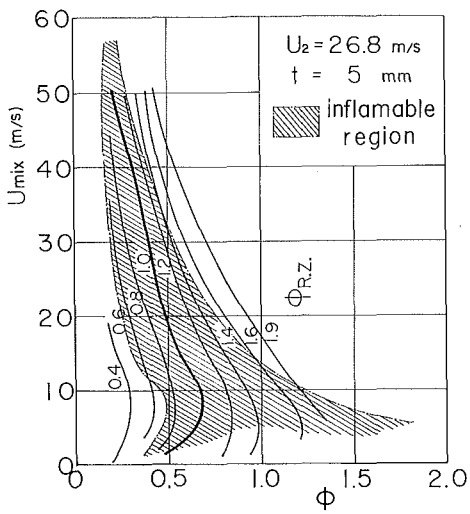

Fig. 20. Constant ϕ_{RZ} diagram.

gradient. And $\phi_{RZ}=1.0$ line is regarded as the axis in the spread of the inflamable region. It can be seen, therefore, that behaviors of the flame have varied dependences on the mixing processes. The figure also shows ϕ_{RZ} increases as U_{mix} increases for fixed t, U_2 and ϕ. Namely, the entrainment of the parallel air increases as U_{mix} increases.

7. Conclusion

The following conclusions are carried out from the experiment described above.

1) In a double concentric jet flame, when the burner rim is of sufficient thickness maximum blow out mixture velocity increases with the increase of parallel air velocity. This phenomenon is in contrast to the result when the rim is thin. The flame is stabilized by the recirculation zone formed behind the thick rim.

2) The recirculation zone, which has strong influence on flame stability, has a peculiar flow pattern with the changing of the center jet and the parallel surrounding flow. Forms of flame are roughly distinguished into inner and outer flame, and have a peculiar temperature and gas component concentration-distribution.

3) Flame front is formed on the face where local mixing ratio is 1.0. The position depends on the true mixing ratio in the recirculation zone.

4) The entrainment rate of the parallel air into the recirculation zone increases as the mixture velocity increases.

Acknowledgement

The authors wish to express their tanks to Dr. S. Fukazawa, Professor, Emeritus Hokkaido Univ. for his useful suggestion for this investigation, and also to E. Saito, S. Kotoura, K. Otaki, K. Hayashi, K. Yamashita for their assistance in the experiments.

References

1) S. B. Reed: Combustion and Flame,11 (1967), 177.
2) H. E. Edmondson, et al.: 12th Symp. (International) on Combustion (1969), p. 1007.
3) A. Saima: Trans. JSME Vol. 26, No. 168 (1960-8).
4) R. Matsumoto et al.: Trans. JSME Vol. 34, No. 263 (1968-7).
5) A. Nomaguchi et al.: Trans. JSME Vol. 39, No. 326 (1974-10).
6) K. Sakai et al.: Journal of Fuel Institute. Vol. 54, No. 582 (1975).
7) E. E. Zukoski, et al.: Comb. Resea. and Revi. ws AGARD (1955), 167.
8) L. A. Povinelli: Combustion and Flame 4 (1960), 355.
9) N. A. Chigier et al.: Trans. ASME (1964-12), 792.
10) E. Minx et al.: VDI-Berichte Nr. 199 (1972).